



# Preparation and properties of LDHs/epoxy nanocomposites

Huai-Bin Hsueh, Chuh-Yung Chen\*

*Department of Chemical Engineering, National Cheng-Kung University, Tainan 70101, Taiwan, ROC*

Received 27 February 2003; received in revised form 20 June 2003; accepted 27 June 2003

## Abstract

Layered double hydroxides (LDHs)/epoxy nanocomposites were prepared by mixing the amino laurate intercalated LDHs, EPON 828 resin, and Jeffamine D400 as a curing agent. The organo-modified LDHs with hydrophobic property easily disperse in epoxy resin, and the amino laurate intercalated LDHs with large gallery space allow the epoxy molecules and the curing agents to easily diffuse into the LDHs galleries at elevated temperature. After the thermal curing process, the exfoliated LDHs/epoxy nanocomposites were formed. X-ray diffraction was used to detect the formation process of the exfoliated LDHs/epoxy nanocomposites. TEM was used to observe the dispersed behavior of the LDHs nanolayers, and the LDHs nanolayers were exfoliated and well dispersed in these nanocomposites. Owing to the reaction between the amine groups of the intercalated amino laurate and epoxy groups, the adhesion between the LDHs nanolayers and epoxy molecules makes these LDHs/epoxy nanocomposites more compatible. Consequently, the tensile properties from tensile test and the mechanical properties from DMA were enhanced, and the  $T_g$  of these nanocomposites from DMA and TMA were increased. Coefficients of thermal expansion (CTEs, below and above  $T_g$ ) of these nanocomposites from TMA decreased with the LDHs content. The thermal stability of these nanocomposites was enhanced by the well dispersed LDHs nanolayers.

© 2003 Elsevier Ltd. All rights reserved.

**Keywords:** Epoxy; Layered double hydroxides; Nanocomposites

## 1. Introduction

Inorganic/organic nanocomposites are composite materials that contain inorganic phases with dimensions under 100 nm [1–3]. Two main approaches to well disperse inorganic fillers in polymer matrices and to produce excellent compatibility between inorganic and organic phases are employed to prepare nanocomposites [4–7]. These approaches dramatically improve their mechanical and thermal properties over those of an unfilled polymer. In comparison of the conventional inorganic/polymer composites with over 30 wt% loading of microscale inorganic-fillers, the enhancements on the inorganic/polymer nanocomposites are achieved with less than 10 wt% loading of the well dispersed nanoscale inorganic-fillers [8–10]. Additionally, the introduction of adhesion between the inorganic and organic phases enhances the compatibility of the nanocomposites, and facilitates stress transfer to the reinforcing phase,

effectively improving the tensile properties and toughness of these nanocomposites [11].

Over the last few years, most researches on nanocomposites have focused on the use of silicate clays as nanoparticles [3,12]. The clays have been studied widely because they are naturally occurring minerals that are commercially available, and exhibit a platy morphology with a high aspect ratio and considerable cation exchange capacity. Clay/polymer nanocomposites, including exfoliated and intercalated types, exhibit improved mechanical properties, barrier properties, thermal stability, resistance to solvent swelling, and lower flammability than pristine polymer and conventional composites. Moreover, exfoliated clay/polymer nanocomposites in which single nanolayers are well dispersed in the polymer matrix outperform intercalated clay/polymer nanocomposites. The morphology and performance of clay/epoxy nanocomposites with various clays have been widely researched [13–16]. The key to achieving exfoliated clay/epoxy nanocomposites is first to load the clay gallery with hydrophobic onium ions; the epoxy and curing agents then diffuse into the gallery, and then a curing process

\* Corresponding author. Tel.: +886-6-2757575x62643; fax: +886-6-2360464.

E-mail address: [ccy7@ccmail.ncku.edu.tw](mailto:ccy7@ccmail.ncku.edu.tw) (C.Y. Chen).

is performed to obtain the nanocomposites. From the past reports, the alkylammonium ions are always used to prepare the organo-clay [3]. The purpose of the intercalation of alkylammonium ions into clays is not only to enlarge the clays galleries, but also to improve hydrophobicity of the clay nanolayers to facilitate exfoliation and disperse them effectively in the epoxy matrix to obtain the exfoliated clay/epoxy nanocomposites. Several reports on clay/epoxy nanocomposites have demonstrated that their glass transition temperatures are lower than that of pristine epoxy [16, 17], perhaps because a lack of adhesion between the clay nanolayers and epoxy molecules causes phase separation, or increases the free volume between them; hence, the unrestrained epoxy molecular chains move easily upon heating.

In this work, the layered double hydroxides (LDHs) described by the formula  $[M(II)_{1-x}M(III)_x(OH)_2]^{x+} \times [A_{x/n}^{n-} \cdot mH_2O]^{x-}$ , where M(II) and M(III) are divalent and trivalent cations, respectively, and  $A^{n-}$  is an exchangeable anion, are chosen as inorganic fillers to prepare LDHs/epoxy nanocomposites. LDHs are natural minerals and synthetic materials with positively charged layers [18,19]. They differ from silicate clays with negatively charged layers. Accordingly, the intercalation characteristics of LDHs and silicate clays involve anionic exchange and cationic exchange, respectively. Few reports in recent years have addressed LDHs/polymer systems [20–23]. Most discussions of LDHs/polymer focused mainly on the intercalation reaction of the polymer molecule chains into the LDHs nanolayers, but the exfoliation reaction and performance of LDHs/polymer systems has been rarely discussed. In the authors' laboratory, exfoliated LDHs/polyimide nanocomposites with excellent mechanical and thermal properties have been briefly reported [24]. In this study, the LDHs with intercalated amino laurate are used to prepare LDHs/epoxy nanocomposites. The intercalation of amino laurate into the LDHs makes the LDHs nanolayers more hydrophobic, enabling them to be exfoliated by epoxy molecules, to generate the exfoliated LDHs/epoxy nanocomposites, which is the same purpose as the preparation of the organoclay for the exfoliated clay/epoxy nanocomposites. Additionally, another important reason for the adoption of amino laurate as the intercalated species is that the reaction between the amine groups of the intercalated amino laurate and epoxy groups generates adhesion between the LDHs nanolayers and epoxy molecules, making the exfoliated LDHs/epoxy more compatible. Consequently, exfoliated LDHs/epoxy nanocomposites with excellent compatibility are expected to show dramatically improved mechanical and thermal properties over those of pristine epoxy. This study briefly discusses the preparation, characterization, and properties of exfoliated LDHs/epoxy nanocomposites.

## 2. Experimental

### 2.1. Materials

The diglycidyl ether of bisphenol A (DGEBA, Shell EPON 828 with a molecular weight of 377) and the curing agent of polyoxypropylene diamine (Jeffamine D400 with a molecular weight of 400, Huntsman Chemicals) were used to prepare the pristine epoxy resin and the LDHs/epoxy nanocomposites.  $Mg(NO_3)_2 \cdot 6H_2O$  (Riedel–deHaen),  $Al(NO_3)_3 \cdot 9H_2O$  (Riedel–deHaen), sodium hydroxide (Riedel–deHaen) and amino lauric acid (TCI) were used to synthesize the amino laurate intercalated layered double hydroxides (LDHs-AL).

### 2.2. Preparation of the layered double hydroxides-amino laurate (LDHs-AL)

The LDHs-amino laurate was prepared by the coprecipitation method. 0.8 g (0.02 mol) of NaOH was dissolved in 200 ml of deionized water, and then, 4.3 g (0.02 mol) of amino lauric acid were added to the sodium hydroxide solution. 5.12 g (0.02 mol) of magnesium nitrate and 3.75 g (0.01 mol) of aluminum nitrate were dissolved in 50 ml of deionized water. The nitrate solution was then added drop wise to the vigorously stirred amino laurate/NaOH solution at room temperature and the pH of the solution was maintained at 10 by the addition of 1 M of NaOH solution. After the addition of the nitrate solution, the mixture was reacted at 80 °C for 16 h. The slurry was then filtered until all the supernatant liquid had been removed. The sample was washed five times by doubly deionized water and dried at 70 °C. In order to minimize contamination with atmospheric  $CO_2$ , the preparation of the LDHs-AL was under a nitrogen purge.

### 2.3. Preparation of the LDHs/epoxy nanocomposites

The pristine epoxy resin was prepared by mixing the epoxy (EPON 828) with the diamine curing agent (Jeffamine D400) at room temperature for 2 h, outgassing the mixture under vacuum, and curing via a thermal schedule (75 °C for 3 h and 135 °C for an additional 3 h). For preparation the exfoliated LDHs/epoxy nanocomposites, the LDHs were added into the epoxy (Epon 828), and the mixture was stirred at 55 °C for 3 h. Then, the diamine curing agent (Jeffamine D400) was added and further mixed with LDHs/epoxy (EPON 828) at room temperature for 2 h. Subsequently, the LDHs/epoxy/curing agent mixture was outgassed under vacuum, followed by curing by the same thermal schedule as that of pristine epoxy. The diamine curing agent (Jeffamine D400) and intercalated amino laurate were counted the same equivalent amounts with epoxy (Epon828) in the preparation of these nanocomposites.

## 2.4. Characterizations and measurements

The X-ray diffraction patterns were recorded on Rigaku RINT2000 X-ray Diffractometer, using Cu K $\alpha$  radiation. FT-IR spectra were obtained with Bio-Rad FTS-40A FT-IR analysis. Carbon, hydrogen and nitrogen analyses were carried out with Heraeus CHN-O-RAPID Elemental Analyzer. Magnesium and aluminum analyses were carried out with HEWLETT PACKARD 4500 Inductively Coupled Plasma-Mass Spectrometer. Solid-state  $^{27}\text{Al}$ -NMR spectrum was obtained on a Bruker AVANCE 400 spectrometer. Microstructural characterizations of the nanocomposites were carried out using Hitachi HF-2000 FE TEM at an acceleration voltage of 200 kV. The tensile strength, elongation, and Young's modulus of the LDHs/epoxy nanocomposites were recorded on an Instron-4464 Universal Tester. The samples were dog-bone-shaped. The results of the tensile properties for five samples were averaged. The dynamic mechanical analysis of the nanocomposites was carried out with Du-Pont 2980 Dynamic Mechanical Analyzer at a heating rate of 5 °C/min. The coefficients of thermal expansion (CTEs) of the nanocomposites were obtained with Du-Pont 2940 Thermal Mechanical Analyzer at a heating rate of 10 °C/min under nitrogen purge. Dynamic Thermogravimetric analysis (TGA) was performed with Perkin Elmer TAC 7/DX at a heating rate of 20 °C/min under nitrogen purge.

## 3. Results and discussion

### 3.1. Characterization of the layered double hydroxides-amino laurate

Fig. 1 shows the FT-IR spectrum of the LDHs-AL. A broad absorption peak between 3600 and 3000  $\text{cm}^{-1}$  is assigned to O–H group stretch of both the hydroxide layers and the interlayer water. Strong absorption peaks of asymmetric and symmetric R–COO $^{-}$  are observed at 1555 and 1399  $\text{cm}^{-1}$ , respectively. The characteristic

peaks of aliphatic C–H stretch are at 2922 and 2852  $\text{cm}^{-1}$ . The peaks of N–H stretch and N–H bend are overlapped with the characteristic peaks of O–H group and R–COO $^{-}$  group, so they are not easily found from the spectrum. Therefore, the weak absorption band for the C–N stretch at 1095 is used to identify the existence of the amine group. These peaks demonstrate that amino laurate was intercalated into the LDHs.

Fig. 2 shows the X-ray patterns and proposed paraffin structure of the LDHs-AL. The observed data shows a basal spacing of 21 Å ( $2\theta = 3.9^\circ$ ) for the LDHs-AL. The space between the Mg/Al nanolayers of the LDHs-AL is larger than that of the unmodified LDHs. The basal spacing of the unmodified LDHs is 7.8 Å.

Fig. 3 shows the  $^{27}\text{Al}$  MAS NMR spectrum of the LDHs-AL. Resonance of octahedrally coordinated aluminum within the brucite-like layers of the LDHs occurs in the range  $-10$  to  $+20$  ppm. The  $^{27}\text{Al}$  MAS NMR spectrum of the LDHs-AL reveals a single resonance at  $+9.4$  ppm, which indicates that all the aluminum atoms are octahedrally coordinated in the LDHs-AL. Thus, the brucite-like layers were successfully prepared within the LDHs-AL.

ICP analysis for the LDHs-AL yielded the following results: Al, 11.0% and Mg, 20.4%. C, H and N analysis yielded the following results: C, 31.74%, H, 7.67%, and N, 3.00%. The empirical formula of the LDHs-AL, determined from the experimental data, is  $\text{Mg}_2\text{Al}_{0.96}(\text{OH})_{2.7}(\text{amino laurate})_{1.1}(\text{CO}_3^{2-})_{0.3} \cdot 2.7\text{H}_2\text{O}$ , which correlates with the Mg:Al ratio (2:1) used to prepare the sample.

### 3.2. Characterization of the exfoliated LDHs/epoxy nanocomposites

The first goal in this work is to synthesize appropriate organo-LDHs for preparing exfoliated and compatible LDHs/epoxy nanocomposites. The intercalation of amino laurate with alkyl chains into the LDHs nanolayers converts hydrophilic LDHs nanolayers into more hydrophobic LDHs nanolayers. This organo-modified process not only enlarges the gallery between the nanolayers, but also improves the

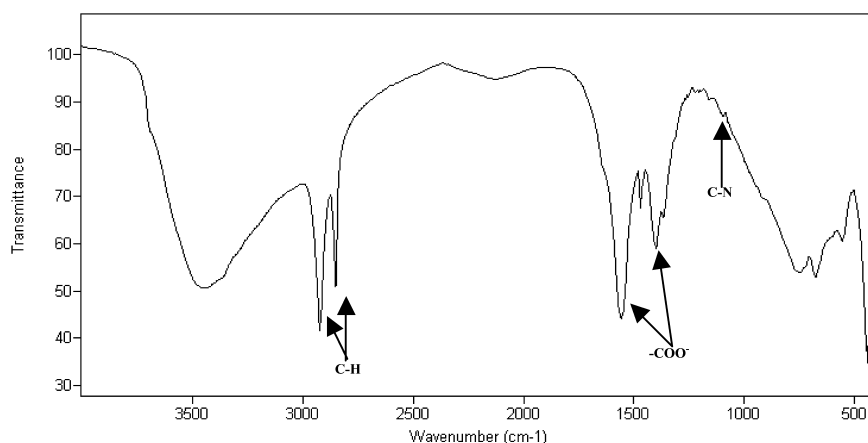


Fig. 1. The FT-IR spectrum of LDHs-AL.

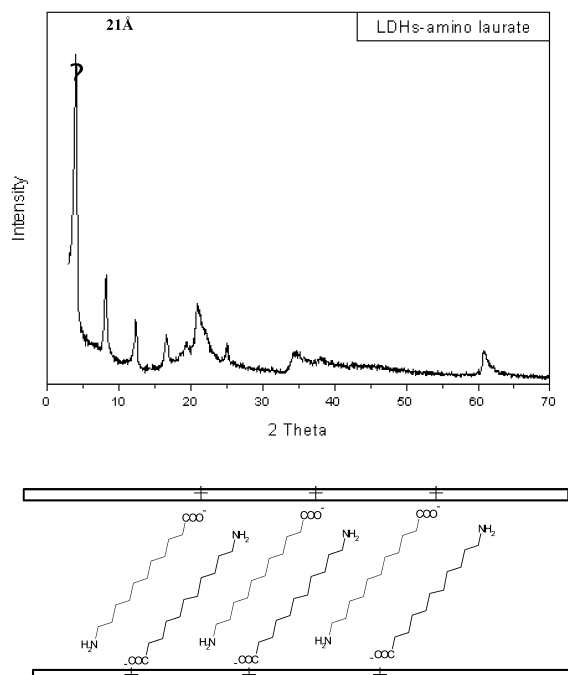


Fig. 2. The X-ray diffraction pattern and the paraffin structure of LDHs-AL.

interfacial properties between the inorganic and organic phases, allowing the epoxy molecules and hydrophobic diamine curing agents to easily diffuse into the gallery to yield the exfoliated LDHs/epoxy nanocomposites. As well as providing hydrophobic environment for the LDHs intragallery, the amine groups of the intercalated amino laurate can react with the epoxy groups to generate adhesion between the LDHs nanolayers and epoxy molecules to form a compatible nanocomposites. Compatible and exfoliated LDHs/epoxy nanocomposites are thus obtained.

In preparing these nanocomposites, LDHs powders were premixed with EPON 828 epoxy resins, and the mixture was stirred at room temperature for 1 h. The LDHs/EPON828 mixture was in a heterogeneous, white state at this stage of mixing. After the temperature was increased to 55 °C, and the mixture stirred at this temperature for 3 h, the mixture became colorless. Fig. 4 shows the FT-IR spectra of the LDHs/EPON 828 mixtures with 5 wt% LDHs loading. The intensity of the 910 cm<sup>-1</sup> characteristic peak that corre-

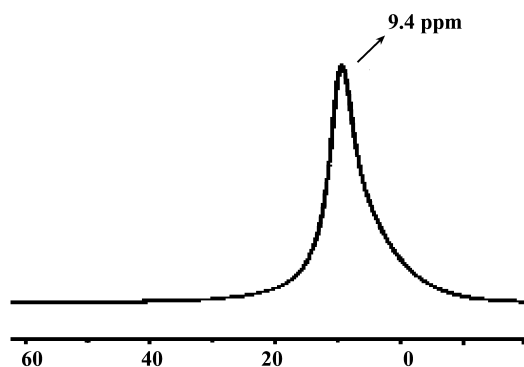


Fig. 3. <sup>27</sup>Al MAS NMR of LDHs-AL.

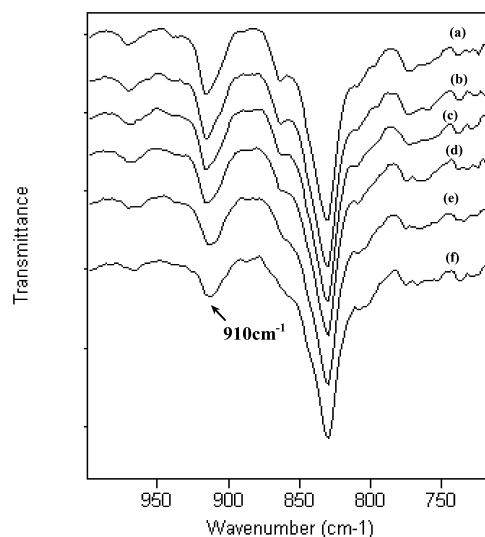


Fig. 4. The FT-IR spectra of LDHs/EPON 828 mixture at different stages: (a) at room temperature for 0 min, (b) at room temperature for 60 min, (c) at 55 °C for 30 min, (d) at 55 °C for 60 min, (e) at 55 °C for 120 min, (f) at 55 °C for 180 min.

sponds to the epoxy group is maintained after stirring at room temperature for 1 h, because no reaction occurred between the epoxy groups and intercalated amino laurate, and a lack of diffusion of epoxy molecules into the LDHs gallery caused the LDHs/EPON 828 mixture to remain heterogeneous and white. At 55 °C, the gradual diminishing of the intensity of the 910 cm<sup>-1</sup> peak reveals that the amine groups of the intercalated amino laurate have reacted with the epoxy groups. The infrared results confirm that the epoxy molecules can diffuse into the LDHs gallery at 55 °C, and that a further chemical reaction occurs in the LDHs gallery. The homogeneously clear LDHs/epoxy mixture is obtained accordingly.

XRD is a powerful technique for detecting the formation and structure of exfoliated LDHs/epoxy nanocomposites because the ordered LDHs nanolayers with the intercalated amino laurate have a lamellar structure. Fig. 5(A) shows the formation of the exfoliated LDHs/epoxy nanocomposites with 5 wt% LDHs loading. At room temperature, no epoxy molecules diffuse into the gallery, which agrees with the infrared results obtained for the LDHs/EPON 828 mixture. At an elevated temperature (55 °C), the space of the LDHs gallery is gradually increased by the diffusion of the epoxy molecules into the LDHs gallery; hence, the 001 diffraction peak shifts toward the low degree region indicating that the intercalated amino laurate starts moving to enable epoxy molecules to penetrate into the gallery at this temperature. Subsequently, the epoxy groups react with the grafted amino laurate, enlarging the gallery allowing more epoxy molecules to diffuse into the gallery. This finding also agrees with the infrared results. Further expansion in the LDHs gallery proceeds when the LDHs/EPON 828 and the curing agent are mixed completely, causing a slight increasing in the LDHs gallery space. In the pre-curing

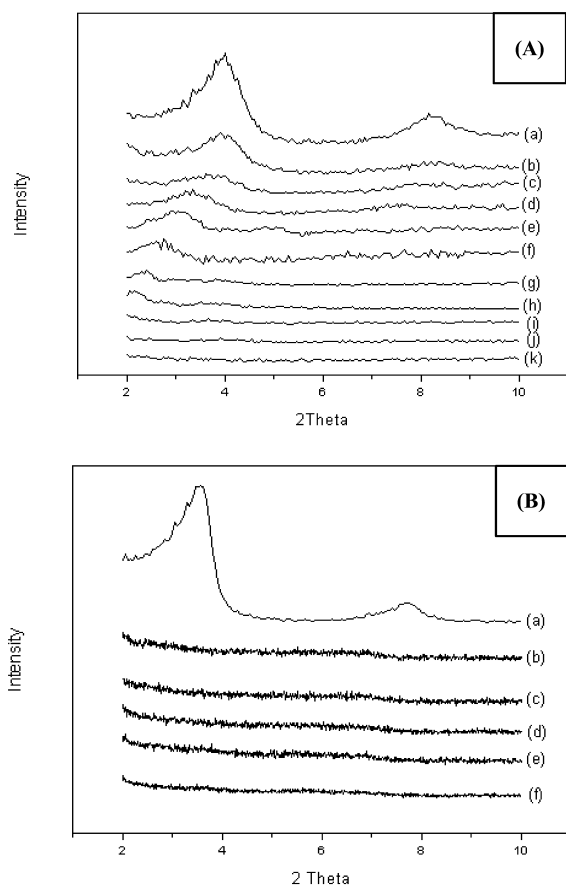


Fig. 5. (A) The X-ray diffraction patterns of (a) LDHs-AL, (b) LDHs/EPON 828 stirred at room temperature for 1 h, (c) LDHs/EPON 828 stirred at 55 °C for 30 min, (d) LDHs/EPON 828 stirred at 55 °C for 60 min, (e) LDHs/EPON 828 stirred at 55 °C for 120 min, (f) LDHs/EPON 828 stirred at 55 °C for 180 min, (g) LDHs/EPON 828/Jeffamine D400 (LDHs/epoxy) stirred at room temperature for 1 h, (h) LDHs/epoxy cured at 75 °C for 30 min, (i) LDHs/epoxy cured at 75 °C for 60 min, (j) LDHs/epoxy cured at 75 °C for 120 min, (k) LDHs/epoxy cured at 135 °C for 30 min, (l) LDHs/epoxy cured at 135 °C for 60 min. (B) The X-ray diffraction patterns of LDHs powder, epoxy resin, and LDHs/epoxy nanocomposites with various LDH-AB contents.

process (75 °C), the further shift of the 001 diffraction peak toward the low degree region indicates that the gallery is gradually expanded by cross-linking polymerization, and then the ordered LDHs nanolayers start losing their regular structure to exfoliate into the epoxy networks. Upon further heating to 135 °C, the absence of the 001 diffraction peak provides strong evidence that the completely cross-linking networks have exfoliated the intercalated LDHs nanolayers during the thermal set curing process to generate the exfoliated LDHs/epoxy nanocomposites. The FT-IR and XRD results thus confirm that the formation of the compatible and exfoliated LDHs/epoxy nanocomposites requires first loading the LDHs gallery with epoxy molecules and then enlarging the LDHs gallery by reacting the epoxy molecules with the intercalated amino laurate. After the curing agents diffuse into the gallery, the cross-linking polymerization gradually disorders the intercalated

LDHs nanolayers, and finally exfoliates the LDHs nanolayers in the epoxy cross-linking networks. Scheme 1 shows the process of formation of the compatible and exfoliated LDHs/epoxy nanocomposites.

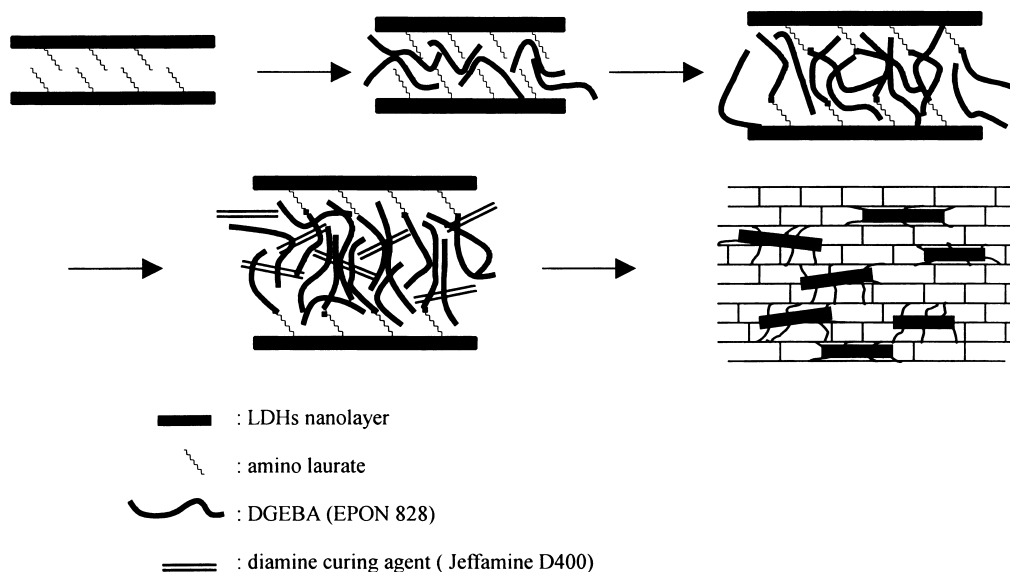
Fig. 5(B) displays the XRD patterns of the LDHs/epoxy nanocomposites with various LDHs contents. The XRD patterns of the LDHs/epoxy nanocomposites, like those of pristine epoxy resin, do not include any 001 diffraction peak after curing, indicating that these nanocomposites have an exfoliated structure. TEM is used to elucidate the dispersed behavior of the exfoliated nanolayers in epoxy networks. Fig. 6 shows TEM micrographs of these exfoliated LDHs/epoxy nanocomposites. The LDHs nanolayers lose their ordered stacking-structure, and are exfoliated in the epoxy matrix. The TEM results are consistent with the XRD results.

The optical transparent property is a significant result for the exfoliated LDHs/epoxy nanocomposites. As shown in Fig. 7, the LDHs/epoxy nanocomposites are transparent as the pristine epoxy resin. This result suggests that the LDHs nanolayers are fully exfoliated in epoxy resin so that single LDHs nanolayer exhibits the nearly same refraction index as the epoxy resin.

### 3.3. Tensile properties

The tensile strength vs. LDHs content curves in Fig. 8 show the benefit of the exfoliated LDHs nanolayers in reinforcing epoxy resin. The tensile strengths of the exfoliated LDHs/epoxy nanocomposites are superior to that of the pristine epoxy. The reaction between the intercalated amino laurate and the epoxy resins provides adhesion between these two phases, promoting their compatibility, reducing the extent of phase separation. Therefore, the tensile strength of these nanocomposites increases with the LDHs content. Fig. 8 shows the Young's moduli of these nanocomposites with various LDHs contents. The tensile modulus for these LDHs/epoxy nanocomposites also increases with LDHs content because the exfoliation of the rigid LDHs nanolayers in epoxy networks directly enhances the stiffness of these nanocomposites, increasing their tensile moduli. Clearly, the tensile properties of the LDHs/epoxy nanocomposites are improved with the loading of LDHs nanolayers, because the exfoliated LDHs nanolayers are thoroughly dispersed in the epoxy networks, and each nanolayer contributes to the reinforcement of the nanocomposites. Interestingly, the participation of the intercalated amino laurate with EPON 828 and Jeffamine D400 in the curing process influences the elasticity of the LDHs/epoxy nanocomposites. As shown in Fig. 8, the elongation at break gradually increases with the LDHs content from 0 to 3 wt% in the exfoliated nanocomposites. When the LDHs content exceeds 3 wt%, the elongation at break is slightly lowered, but is still higher than that of pristine epoxy. Typically, composites reinforced by inorganic fillers exhibit a lower elasticity than pristine





Scheme 1. The formation process of the LDHs/epoxy nanocomposites.

polymer. The increase in the elongation at break of the exfoliated LDHs/epoxy nanocomposites has two causes. (1) The adhesion between the inorganic and organic phases is enhanced by a reaction between the intercalated amino laurate and the epoxy resins, which makes these nanocomposites less easy to break during extension. (2) The long alkyl chain of the intercalated amino laurate plasticizes the exfoliated LDHs/epoxy nanocomposites. Accordingly, exfoliated LDHs/epoxy nanocomposites with excellent compatibility exhibit enhanced tensile properties including tensile strength, Young's modulus, and elongation at break.

### 3.4. Viscoelastic properties

Dynamic mechanical analysis (DMA) determines the storage modulus ( $E'$ ), the loss modulus ( $E''$ ), and the loss factor ( $\tan \delta$ ) as functions of temperature. The storage modulus reflects the elastic modulus of the nanocomposites, and the loss modulus is related to the energy lost due to the friction associated with the motion of the polymer chain. Fig. 9 shows that the storage modulus of these nanocomposites increases with the LDHs content. When the LDHs nanolayers are exfoliated and thoroughly dispersed in the epoxy networks, the rigid LDHs nanolayers directly enhance the stiffness of these LDHs/epoxy nanocomposites. Therefore, the storage modulus of these nanocomposites exceeds that of pristine epoxy. Fig. 9 shows the loss moduli and the glass transition temperatures (at the maximum of the loss modulus peak) of these nanocomposites. The loss modulus of these nanocomposites also slightly increases with the LDHs content, because the exfoliation of the LDHs nanolayers increases the friction between the LDHs nanolayers and the epoxy molecules as the temperature increases. The loss modulus is considered in the temperature range from  $-100$  to  $100$  °C to elucidate the effect of

exfoliated LDHs nanolayers on the  $\alpha$ -transition and  $\beta$ -transition of these nanocomposites. The  $\alpha$ -transition is related to the Brownian motion of the main chains of the epoxy networks at the transition from the glassy to the rubbery state, which determines the glass transition temperatures of these nanocomposites. The  $\beta$ -transition occurs at a lower temperature and is related to the crankshaft rotation of the hydroxy ether segments of the epoxy networks in the glassy state. In the preparation of LDHs/epoxy nanocomposites, the reaction between the intercalated amino laurate and the epoxy resins produces the adhesion between the exfoliated LDHs nanolayers and epoxy networks. Upon heating, the mobility of the main chains of the epoxy resins is restrained by the nanolayers by the adhesion between these two phases; hence, the polymer undergoes high temperature relaxation,  $\alpha$ -transition, causing the glass transition temperature of these nanocomposites to increase with the LDHs content. This figure also shows that the broad range of temperature over which the  $\beta$ -transition occurs shifts slightly upwards, because hydrogen bonds form between the hydroxy groups of the hydroxy ether segments of the epoxy resins and the surfaces of the LDHs nanolayers, retarding the motion of the hydroxy ether segments, and causing the  $\beta$ -transition to shift slightly toward the high temperature region.

Fig. 9 shows the temperature dependence of  $\tan \delta$  of the LDHs/epoxy nanocomposites. The loss factor  $\tan \delta$  is the ratio of the loss modulus to the storage modulus, and is very sensitive to the structural transformation of the materials. The  $\tan \delta$  peak also can be used to identify  $T_g$  of these nanocomposites, which shifts to high temperature as the tendency of the maximum loss modulus peak ( $\alpha$ -transition) of these nanocomposites. This figure shows that increasing the LDHs content reduces the height of the  $\tan \delta$  peak, which is related to the energy damping characteristics of the

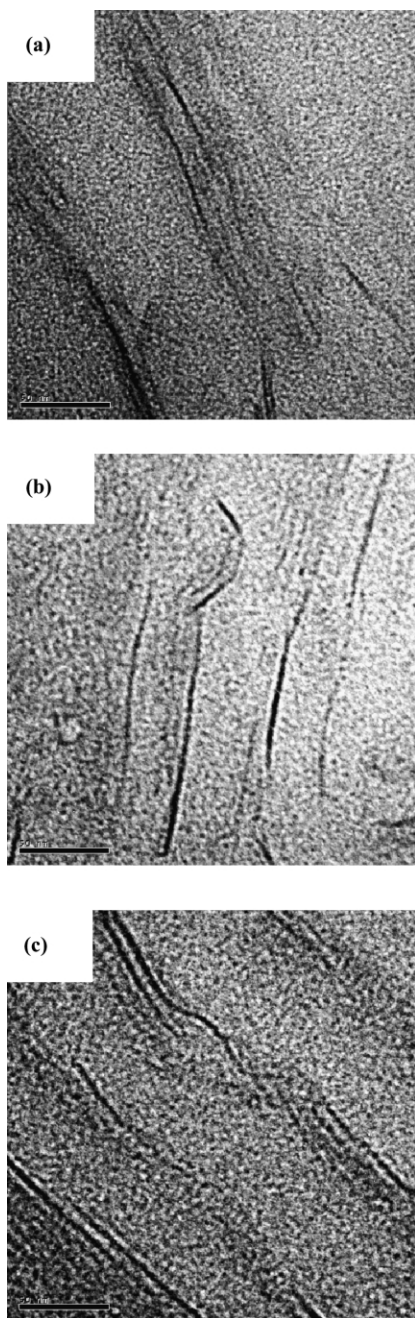


Fig. 6. TEM micrographs of LDHs/epoxy nanocomposites with various LDHs contents: (a) 3 wt%, (b) 5 wt%, and (c) 7 wt%. The bar length is 50 nm.

materials. The height of the  $\tan \delta$  peak decreases as the LDHs content increases because the stiffness of these exfoliated LDHs/epoxy nanocomposites is enhanced by the rigid LDHs nanolayers which are effectively dispersed in epoxy networks. The broadness of the  $\tan \delta$  peak is determined at the half of its height, and is indicative of the relaxation of the polymer chain with increasing temperature. The broadness of the  $\tan \delta$  peaks of these nanocomposites slightly increases from 16 °C for pristine epoxy to 19 °C for the LDHs/epoxy nanocomposites with

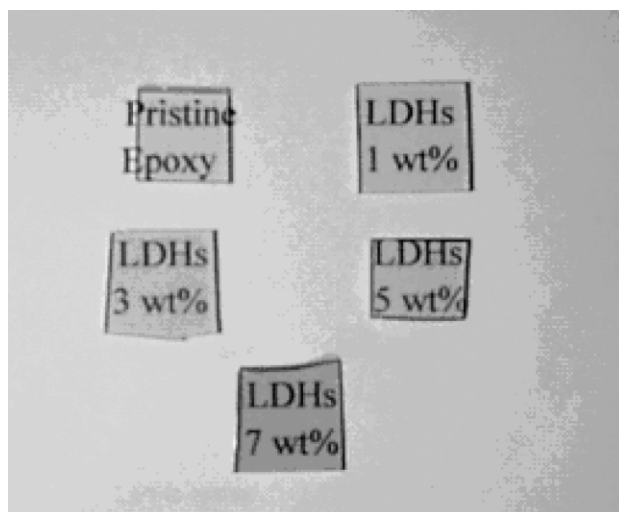


Fig. 7. Optical images of the pristine epoxy resin and the LDHs/epoxy nanocomposites with various LDHs contents. The thickness of each sample is about 3 mm.

7 wt% LDHs loading because the adhesion between the LDHs nanolayers and epoxy molecules attaches the epoxy molecules to the LDHs nanolayers, reducing the mobility of the main chain of the epoxy molecules as the temperature increases. Consequently, the  $\tan \delta$  peak of the LDHs/epoxy nanocomposites covers a slightly wider temperature range than that of pristine epoxy. The DMA results indicate that the exfoliated LDHs nanolayers effectively enhance the mechanical properties of the LDHs/epoxy nanocomposites.

### 3.5. Thermal expansion properties

Fig. 10 plots the dimensional change vs. temperature curves for the exfoliated LDHs/epoxy nanocomposites. Fig. 11 shows that the CTEs below and above  $T_g$  for the LDHs/epoxy nanocomposites decrease as the LDHs content increases. The inorganic LDHs nanolayers neither easily deform nor relax like the organic epoxy molecules as the temperature increases. Therefore, given effective dispersion of the exfoliated LDHs nanolayers in the epoxy matrix, the rigid LDHs nanolayers effectively retard the thermal expansion of the epoxy molecules upon heating, causing the CTEs both below and above  $T_g$  of the LDHs/epoxy nanocomposites lower than those of the pristine epoxy resin. The authors' previous report on the effect of LDHs on the CTEs of polyimide revealed that a CTE above  $T_g$  for LDHs/polyimide nanocomposites dramatically decreases as LDHs content increases [24]. In this study, the decrease in the CTE above  $T_g$  for the LDHs/epoxy nanocomposites is much less than that for LDHs/polyimide nanocomposites because above  $T_g$ , the cross-linking epoxy resin possesses a higher dimensional stability than the linear polyimide polymer, such that the effect of LDHs on the CTE above  $T_g$  for the cross-linking epoxy resin is lower.

In exfoliated LDHs/epoxy nanocomposites, the adhesion between the LDHs nanolayers and epoxy molecules pulls

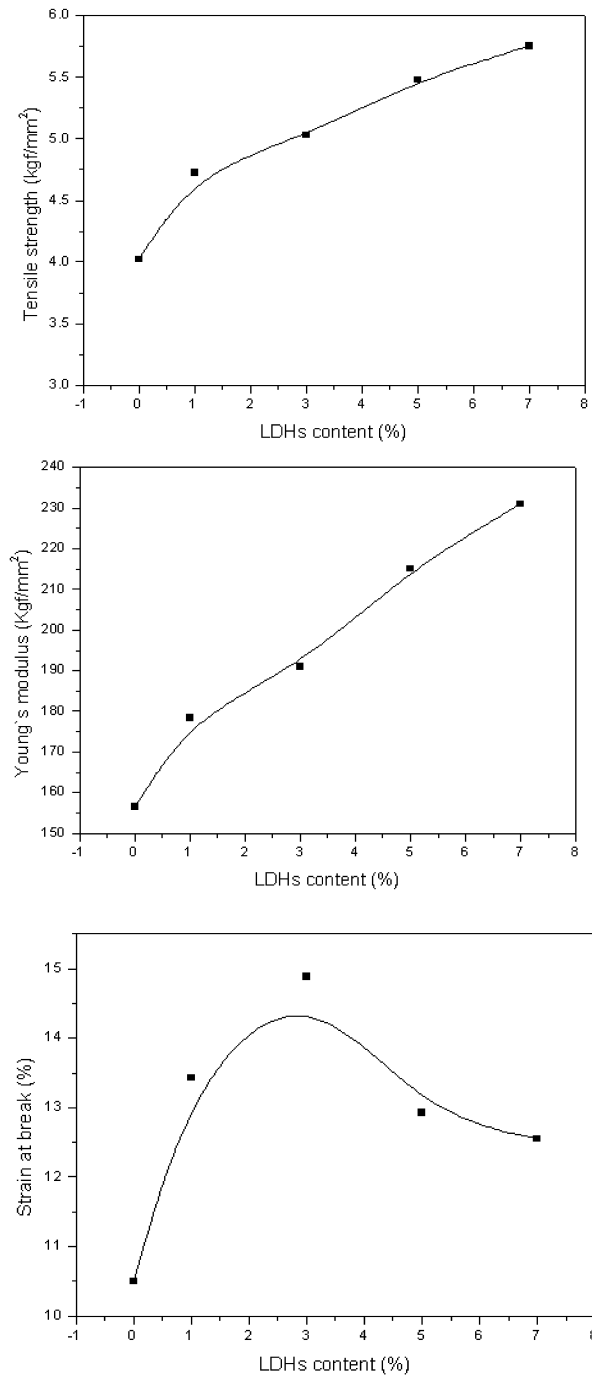


Fig. 8. Effect of the LDHs content on the tensile properties (tensile strength, Young's modulus and strain-at-break) of the LDHs/epoxy nanocomposites.

the epoxy main chains and LDHs nanolayers close together, raising the onset glass transition temperature, as shown in Fig. 10. This tendency corresponds to  $T_g$  obtained from the loss modulus results above. As the LDHs content increases, the rigid LDHs nanolayers dramatically enhance the stiffness of the exfoliated LDHs/epoxy nanocomposites, wherein the extensive segments of the epoxy main chain are not very mobile, greatly broadening the transition region, as also shown in Fig. 10.

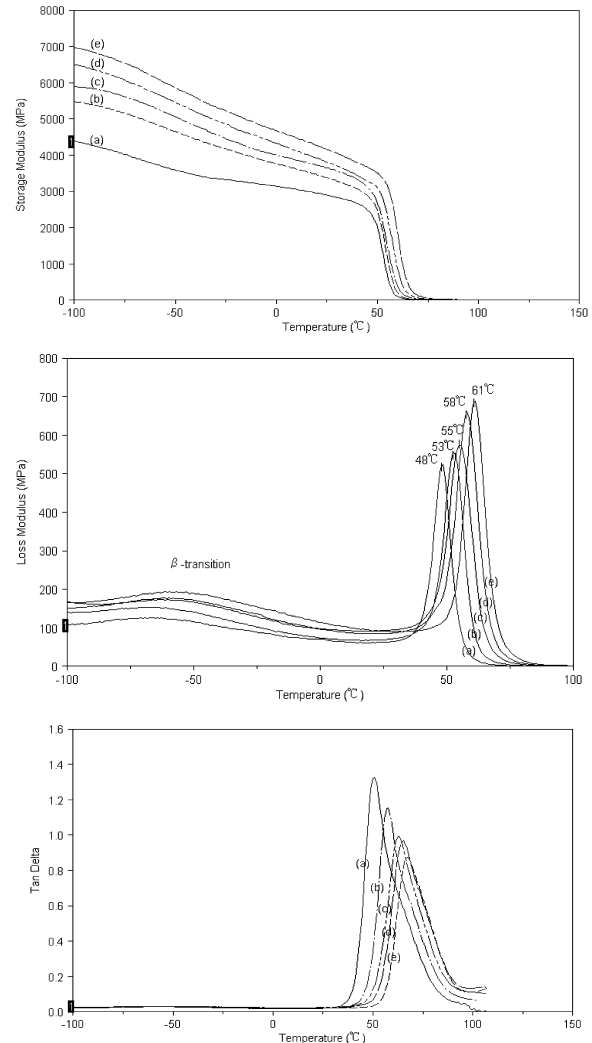


Fig. 9. Storage modulus ( $E'$ ), loss modulus ( $E''$ ) and  $\tan \delta$  of the LDHs/epoxy nanocomposites with various LDHs contents: (a) 0 wt%, (b) 1 wt%, (c) 3 wt%, (d) 5 wt%, (e) 7 wt%.

### 3.6. Thermal stability

Fig. 12 shows thermal stability of exfoliated LDHs/epoxy nanocomposites, by plotting the nanocomposites' weight loss due to volatilization of degraded products as a

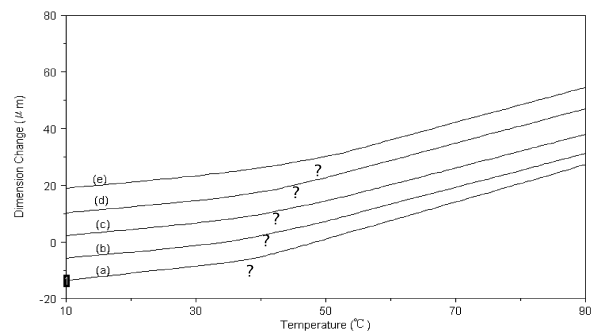


Fig. 10. Dimensional change vs. temperature curves of LDHs/epoxy nanocomposites with various LDHs contents: (a) 0 wt%, (b) 1 wt%, (c) 3 wt%, (d) 5 wt%, (e) 7 wt%.



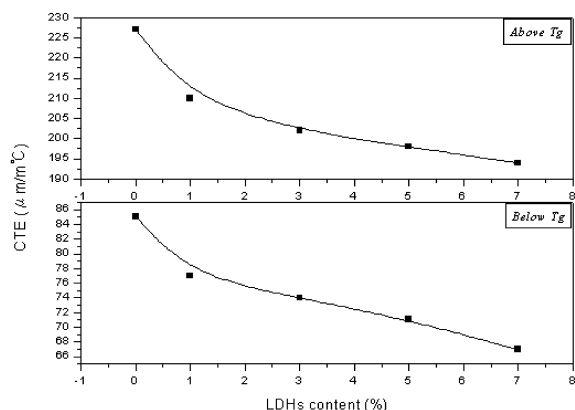


Fig. 11. Effect of LDHs content on the CTEs of LDHs/epoxy nanocomposites.

function of temperature. The results indicate that 7 wt% LDHs loaded nanocomposite degrades at temperature 23 °C above the degradation temperature of pristine epoxy resins. For the exfoliated LDHs/epoxy nanocomposites with good compatibility, not only the difference in chemical structure from the pristine epoxy resin, but also the restrictedly thermal motion of the epoxy molecules by LDHs nanolayers make these LDHs-filled nanocomposites to own the better thermal stability than the pristine epoxy resin. Additionally, the enhanced thermal stability is also attributable to the prevented out-diffusion of the volatile gas from the thermal decomposed products because the exfoliated LDHs nanolayers, well dispersed in epoxy networks, act as the gas barriers, reducing the permeability of the volatile gas.

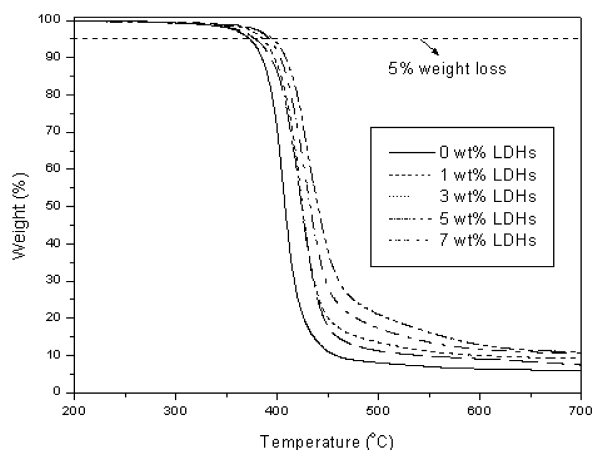


Fig. 12. TGA curves of LDHs/epoxy nanocomposites with various LDHs contents.

Therefore, the dispersion of exfoliated LDHs nanolayers effectively enhances the thermal stability of these nanocomposites.

#### 4. Conclusions

The coprecipitation method was used to synthesize the organo-modified LDHs. The LDHs were prepared by the intercalation of the amino laurate into the LDHs galleries. The exfoliated LDHs/epoxy nanocomposites were successfully prepared by exfoliating the LDHs nanolayers in epoxy matrix. The reaction between the intercalated amino laurate and epoxy groups provided the adhesion between the LDHs nanolayers and epoxy molecules to improve the compatibility between them. Therefore, the exfoliated LDHs/epoxy nanocomposites with excellent compatibility possessed enhanced thermal and mechanical properties as compared to the pristine epoxy resin.

#### References

- [1] Novak BM. *Adv Mater* 1993;5:422.
- [2] Frisch HL, Mark JE. *Chem Mater* 1996;8:1735.
- [3] Pinnavaia TJ, Beall GW. *Polymer-clay nanocomposites*. New York: Wiley; 2000.
- [4] Yang Y, Zhu ZK, Yin J, Wang XY, Oi ZE. *Polymer* 1999;40:4407.
- [5] Ishida H, Campell S, Blackwell J. *Chem Mater* 2000;12:1260.
- [6] Chen Y, Iroh JO. *Chem Mater* 1999;11:1218.
- [7] Mascia L, Kioul A. *Polymer* 1995;36:3649.
- [8] Okada A, Usuki A, Kurauchi T. *Hybrid organic-inorganic composites*. ACS Symp Ser 1995;55:585.
- [9] Kojima Y, Usuki A, Kawasumi M. *J Mater Res* 1993;8:1185.
- [10] Kojima Y, Usuki A, Kawasumi M. *J Appl Polym Sci* 1993;49:1259.
- [11] LeBaron PC, Wang Z, Pinnavaia TJ. *Appl Clay Sci* 1999;15:11.
- [12] Alexandre M, Dubios P. *Mater Sci Engng* 2000;28:1.
- [13] Wang MS, Pinnavaia TJ. *Chem Mater* 1994;6:468.
- [14] Lan T, Kaviratna PD, Pinnavaia TJ. *Chem Mater* 1995;7:2144.
- [15] Messersmith PB, Giannelis EP. *Chem Mater* 1994;6:1719.
- [16] Triantafillidis CS, LeBaron PC, Pinnavaia TJ. *Chem Mater* 2002;14:4088.
- [17] Becker O, Varley R, Simon G. *Polymer* 2002;43:4365.
- [18] Miyata S. *Clays Clay Miner* 1975;23:369.
- [19] Ulibarri MA, Pavlovic I, Barriga C, Hermosin MC, Cornejo J. *Appl Clay Sci* 2001;18:17.
- [20] Sugahara Y, Yokoyama N, Kuroda K, Kato C. *Ceram Int* 1998;14:163.
- [21] Tanaka M, Park IY, Kuroda K, Kato C. *Bull Chem Soc Jpn* 1989;62:3442.
- [22] Oriakhi CO, Farr IV, Lerner MM. *J Mater Chem* 1996;6:103.
- [23] Leroux F, Besse JP. *Chem Mater* 1994;4:99.
- [24] Hsueh HB, Chen CH. *Polymer* 2003;44:1151.